

## Galactic dust polarized emission at high latitudes and CMB polarization

S. K. Sethi<sup>2</sup>, S. Prunet<sup>1</sup>, F.R. Bouchet<sup>2</sup>

<sup>1</sup>*IAS, bât. 121, 91405 Orsay*

<sup>2</sup>*IAP, 98bis Boulevard Arago, 75014 Paris*



We estimate the dust polarized emission in our galaxy at high galactic latitudes, which is the dominant foreground for measuring CMB polarization using the high frequency instrument (HFI) aboard Planck surveyor. We compare it with the level of CMB polarization and conclude that, for angular scales  $\leq 1^\circ$ , the scalar-induced CMB polarization and temperature-polarization cross-correlation are much larger than the foreground level at  $\nu \simeq 100$  GHz. The tensor-induced signals seem to be at best comparable to the foreground level.

### 1 Introduction

The forthcoming satellite CMB projects MAP and Planck surveyor hold great promise for detecting the CMB polarization. A major stumbling block this detection is the unknown level of galactic polarized foregrounds. In this paper, we attempt to estimate the level of dust polarized emission at high galactic latitudes. We model this emission using the three-dimensional HI maps of the Leiden/Dwingeloo survey at high galactic latitudes and the fact that the dust emission, for a wide range of wavelengths, has a tight correlation with the HI emission maps of this survey<sup>1</sup>. Assuming the dust grains to be oblate with axis ratio  $\simeq 2/3$ , which recent studies support<sup>2</sup>, we determine the intrinsic dust polarized emissivity. The distribution of magnetic field with respect to the dust grain distribution is quite uncertain, we thus consider three extreme cases (to be described below).

### 2 Method

From the HI maps of Leiden/Dwingeloo survey<sup>3</sup> one can construct a statistical model of the three-dimensional dust distribution using the relation between the optical depth for dust emission  $\tau$

at  $\lambda = 250 \mu\text{m}$  and the HI column density  $N_{\text{HI}}$ <sup>1</sup>:

$$\frac{\tau}{N_{\text{HI}}} = 10^{-25} \text{ cm}^2 \quad (1)$$

Boulanger *et al.*<sup>1</sup> also showed that the galactic dust emission spectrum can be well fitted with a Planck spectrum with temperature = 17.5 K with emissivity proportional to  $\nu^2$ . We use this spectral dependence of dust emission throughout this paper. The  $N_{\text{HI}}-\tau$  correlation remains good for  $N_{\text{HI}} \leq 5 \times 10^{20} \text{ cm}^{-2}$  which is typical for high galactic latitudes.

As our aim is to construct two-dimensional maps of polarized component of dust emission from these three-dimensional maps of unpolarized emission, we need the following information: (a) the intrinsic dust polarized emissivity, which depends on the type and shape of the grain, (b) the strength and direction of magnetic field in the diffuse cloud, and (c) the polarization reduction factor.

*Intrinsic polarized emissivity.* The galactic distribution of dust grains can be well understood by the silicate/graphite model, with the volume fraction of graphite between 0.25 and 0.5 of the silicates in the total grain volume<sup>4</sup>. Assuming spheroidal grains, Hildebrand and Dragovan<sup>2</sup> showed that the grains are oblate with the ratio of axis  $\simeq 2/3$ . Assuming no reduction of polarization, the intrinsic polarized emissivity is  $\simeq 30\%$  in this case.

*Magnetic field.* The dust grains align themselves with the magnetic field. To estimate the reduction of polarization from smearing along any line of sight, one needs to know the direction and strength of the magnetic field. There is great uncertainty in the direction of the magnetic field relative to dust distribution as the observational evidence show contradictory indications<sup>5,6</sup>. Therefore, we consider three extreme cases:

- (1) The magnetic field is aligned with the major axis of the structure. This case is relevant for dust filaments aligned with the field.
- (2) The magnetic field lies in the plane perpendicular to the major axis of the structure, with its direction random in that plane (valid e.g. for helicoidal field around filaments)
- (3) The magnetic field has the same direction throughout the three-dimensional map.

Also we assume, as recent observations and theoretical estimates show, that the the dust grains are aligned with the magnetic field independent of the strength of the magnetic field.

*Polarization reduction factor.* The reduction of intrinsic polarized emissivity due to projection on the sky can be written as<sup>4</sup>:

$$\Phi = RF \cos^2 \gamma, \quad (2)$$

where  $R$  is the Rayleigh reduction factor which gives the reduction of polarization due to the inclination of grain axes about the direction of the magnetic field. As discussed above, we assume perfect alignment of the dust grains with the magnetic field and therefore take  $R = 1$  throughout. The  $\cos^2 \gamma$  factor accounts for the projection of the direction of polarization on the plane of the sky. Using the three-dimensional maps, we calculate this factor by first estimating, for every pixel, the direction of the structure by finding the direction of minimum gradient in the nearest 27 pixels in the four nearest velocity templates, which are taken as slices in 3-dimensional space. After finding the direction of dust structure with respect to the plane of the velocity template, the direction of magnetic field can be fixed for Case (1) and (2) of the magnetic field distribution. The  $\cos^2 \gamma$  term ( $\gamma$  being the angle between the direction of magnetic field and the plane of the velocity template) can then be easily computed; and by multiplying by this factor, the projected distribution of polarized emission is evaluated for every velocity template. This procedure is used to construct the projected distribution of the Stoke's parameters for the first two cases of the magnetic field distribution. For the third case (the magnetic field having the same direction

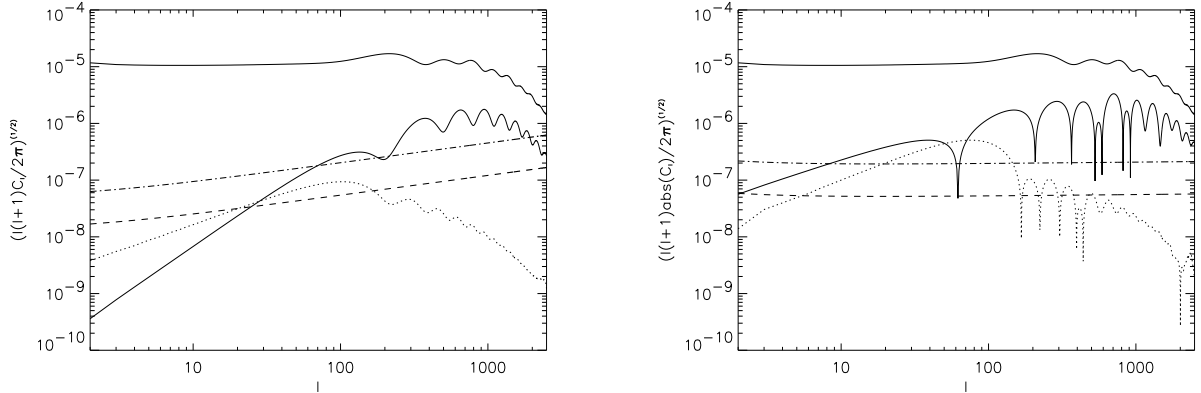


Figure 1: Left Panel: The power spectra of dust polarized emission is compared with the theoretical predictions for CMB polarization. The scalar and tensor-induced E-mode power spectra (*solid* and *dotted* lines respectively) are plotted against the dust polarized power spectra at 143 GHz and 217 GHz (the *dashed* and *dot-dashed* lines, respectively). The CMB temperature power spectrum is shown for comparison (*thick solid* line). The power spectra are plotted in the units of  $\Delta T/T$ . Right Panel: Same as the left panel for the *ET* cross-correlation

everywhere), we assume, for simplicity,  $\cos^2 \gamma = 0.5$ .  $F$  term is the reduction of polarization from summing the contribution of different directions of polarization along any line of sight<sup>7</sup>. This factor is estimated directly by vectorially adding the contribution from every velocity template along a line of sight.

### 3 Results

#### 3.1 Angular distribution of dust polarized emission and comparison with CMB power spectra

We construct two-dimensional  $15^\circ \times 15^\circ$  maps between latitudes  $30^\circ$  and  $75^\circ$  using the methods described in the last section, and take the Fourier transform of these maps to obtain the power spectra of the Stoke's parameters. For a comparison with the CMB polarized component, it is convenient to define variables  $E$  and  $B$ <sup>10</sup>, which are linear combinations of the usual Stoke's parameters in Fourier space. It is because  $B$  always vanishes for the scalar-induced CMB polarization. Also the cross-correlation of  $B$  with all the other variables vanishes.

In terms of these variables, the estimated power spectra and the cross-correlation of dust polarized emission can approximately be fitted by:

$$C_E(\ell) = 8.9 \times 10^{-4} \ell^{-1.3} (\mu\text{K})^2 \quad (3)$$

$$C_B(\ell) = 1.0 \times 10^{-3} \ell^{-1.4} (\mu\text{K})^2 \quad (4)$$

$$C_{ET}(\ell) = 1.7 \times 10^{-2} \ell^{-1.95} (\mu\text{K})^2. \quad (5)$$

The power spectra are normalized at 100 GHz and are for the maps between galactic latitudes  $30^\circ$  and  $45^\circ$  (where the level of contamination is the highest) for Case (1) of the magnetic field distribution. The other two cases of magnetic field distribution result in smaller or comparable level of foregrounds at  $\ell \geq 200$  (for details, see Prunet *et al*<sup>8</sup>).

We plot these against the scalar and tensor induced CMB power spectra for various variables in Fig. 1 and 2. The cosmological model we adopted to compute the CMB spectra is a flat, tilted CDM model, which generates tensor-induced B-mode polarization, with scalar spectral index  $n_s = 0.9$ . We take the tensor spectral index  $n_t = 1 - n_s = 0.1$  with scalar to tensor quadrupole ratio of  $7(1 - n_s)$ . The CMB power spectra were computed using the CMB Boltzmann code CMBFAST<sup>10</sup>.

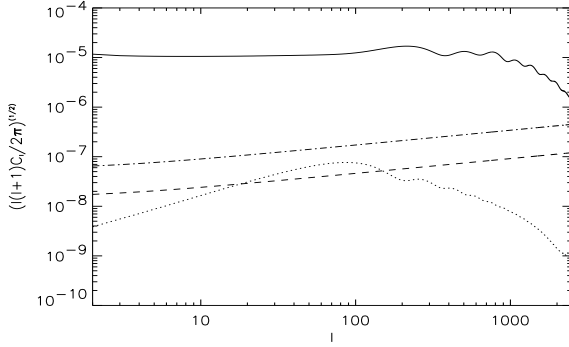


Figure 2: Same as Fig. 1 for B-mode power spectra.

In Fig. 1, the scalar-induced E-mode CMB power spectrum is seen to be above the level of dust contamination for  $\ell \gtrsim 200$  for the two HFI frequency channels at 143 GHz and 217 GHz. However the tensor-induced E-mode CMB fluctuations, which in any case constitute a small part of the E-mode signal, are likely to be swamped by the foreground contamination. The detection of B-mode anisotropies is more interesting as it would unambiguously determine the presence of tensor-induced component in CMB fluctuations<sup>9,11,12</sup>. As seen in Fig. 2 the B-mode power spectrum is at best comparable to the foreground level in a small  $\ell$ -range. Fig 1 shows that the CMB  $ET$  cross-correlation power spectrum from scalar perturbations is more than an order of magnitude above the level of foreground contamination, at least for  $\ell \gtrsim 100$  while the tensor-induced  $ET$  cross-correlation remains below the foreground signal.

As the foregrounds differ from CMB in both  $\nu$ - and  $\ell$ -dependence, the level of foreground contamination can be substantially reduced even in the presence of noise<sup>13,14</sup>. The extension of this technique to include polarization and temperature-polarization cross-correlation, and how it can be used to quantify errors on various power spectra, is described in a companion paper in this volume<sup>15</sup>.

## References

1. F. Boulanger *et al.* , A & A **312**, 256 (1996)
2. R. H. Hildebrand and M. Dragovan, ApJ **450**, 663 (1995)
3. D. Hartmann and W. B. Burton, Atlas of Galactic HI emission, Cambridge University Press (1995)
4. H. M. Lee and B. T. Draine, ApJ **290**, 211 (1985)
5. P. C. Myers and A. A. Goodman, ApJ **373**, 509 (1991)
6. A. A. Goodman, P. Bastien, F. Menard, and P. C. Myers, ApJ **359**, 363 (1990)
7. B. J. Burn, MNRAS **133**, 67 (1966)
8. S. Prunet, S. K. Sethi, and F. R. Bouchet, submitted for publication
9. U. Seljak, ApJ **482**, 6 (1997)
10. U. Seljak and M. Zaldarriaga, ApJ **469**, 437 (1996)
11. M. Kamionkowski and A. Kosowsky, astro-ph/9705219
12. M. Zaldarriaga and U. Seljak, astro-ph/9609170
13. F. R. Bouchet *et al.* , Space Science Rev. 74, 37(1995).
14. M. Tegmark and G. Efstathiou, ApJ **281**, 1297 (1996).
15. S. Prunet, S. K. Sethi, and F. R. Bouchet, this volume.